

## STUDY OF RADIATION FROM RF CAVITIES

R. Sandström, Geneva University, Geneva, Switzerland, also NIKHEF, Amsterdam, The Netherlands  
 D. Huang, Illinois Institute of Technology, Chicago, IL, USA, J. Norem, ANL, Argonne, IL, USA

### Abstract

Essential for muon accelerators such as neutrino factories or muon colliders, ionization cooling channels use RF cavities to restore the energy lost in liquid hydrogen absorbers. One major limitation in cooling comes from electrons emitted from the cavities which can cause breakdowns or unacceptable thermal load to the liquid hydrogen vessels. In the Muon Ionization Cooling Experiment MICE, these electrons also cause background in the detectors. This paper presents simulations related to these dark currents, and analysis of data from a direct measurement of this radiation in the MuCool Test Area (MTA).

### FIELD EMISSION

At local field gradients of 6–8 GV/m the tensile stress becomes equal to the tensile strength of copper, and the material fails which results in a breakdown event [1, 2]. Field emission occurs just below the point where the material fails due to tensile stress, and can be expressed using the Fowler-Nordheim equation

$$n_e^{FN}(E_{surf}) = \frac{A(\beta_{FN}E_{surf})^2}{\phi} \exp\left(-\frac{B\phi^{3/2}}{\beta_{FN}E_{surf}}\right) \quad (1)$$

where  $E_{surf}$  is the surface electric field gradient, while  $A$  and  $B$  are constants [3]. The work function  $\phi$  is the energy required to move an electron from a metal to a point immediately outside its surface, while

$$\beta_{FN} = \frac{E_{local}}{E_{surf}} \quad (2)$$

is a local field enhancement factor due to impurities and asperities of the surface. This model assumes that the free electron model is valid in the metal and that the temperature is zero Kelvin.

### ACCELERATION

Assuming that all electrons are emitted at peak gradient, the emitted electrons are accelerated to a monochromatic kinetic energy. This assumption is justified by the steepness of Eq. (1) at high local gradients. As Fig. 1 illustrates, there is a sharp cut off at low gradients. This effect is due to that the particle is not accelerated enough to reach the opposite side of the cavity before it is decelerated by the oscillating field.

### PHOTON TO ELECTRON RATIO

At the far side of the MTA prototype 201.25 MHz cavity there is a 0.635 cm thick copper plate, followed by 3.8 cm

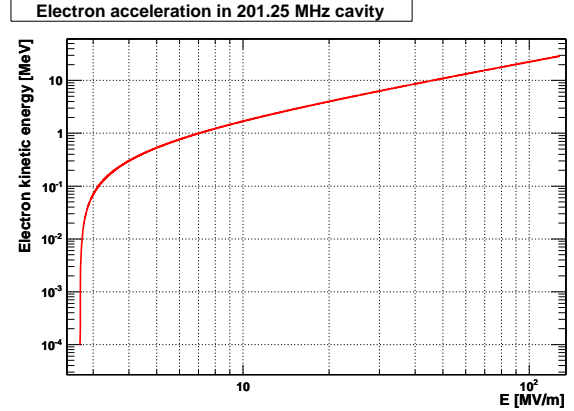


Figure 1: Electron acceleration as a function of electric field gradient in one 201.25 MHz cavity. Calculated in numerically in Matlab.

of aluminum. A NaI detector is placed 4.4 cm from the cavity. As the electrons hit the copper plate they lose energy primarily by ionisation, but also by bremsstrahlung. The bremsstrahlung photons are the primary source of radiation from RF cavities. The radiation yield increases with energy, thus with increasing electric field gradient.

The cross section for an electron of kinetic energy  $T$  to produce a photon with energy  $t$  is

$$\frac{d\sigma}{dt} \approx \frac{A}{X_0 N t} \frac{f(x)}{\int_0^1 f(x) dx}, \quad x \equiv \frac{t}{T}. \quad (3)$$

Traditionally  $f(x) = 1 - x + 0.75x^2$  is used [4], but a fit on Seltzer-Berger parameterized cross section [5] for  $T = 1$  MeV with a 3<sup>rd</sup> degree polynomial shows a better agreement with data ( $\chi^2/\text{ndf} = 0.021/9$ ). With the definition of radiation yield

$$p_y \equiv \frac{\langle t \rangle}{T} = \frac{1}{T} \int_0^T t \frac{d\sigma}{dt} dt \quad (4)$$

the probability density function for an electron to create a photon with fractional energy  $x$  is thus

$$p_{gen}(x) = \frac{p_y}{x} \frac{f(x)}{\int_0^1 f(x) dx}. \quad (5)$$

The radiation yield is taken from interpolations of NIST data, which use the same parameterization [5]. Since the shape  $f(x)$  is fixed to that of  $T = 1$  MeV, an error is introduced when applied to extreme energies. However, this bias is always less than 1.4% in the scope of this paper.

In addition, the photon energy increases with increasing  $T$ , and thus also the probability of exceeding a detector

threshold. Since the cross section for photoelectric effect decreases with increased energy, the transmission of photons through a metal also increases. For high energy photons the transmission to the detector is approximately 40% in the MTA setup, while the infrared divergence at low energy is canceled by the photoelectric effect.

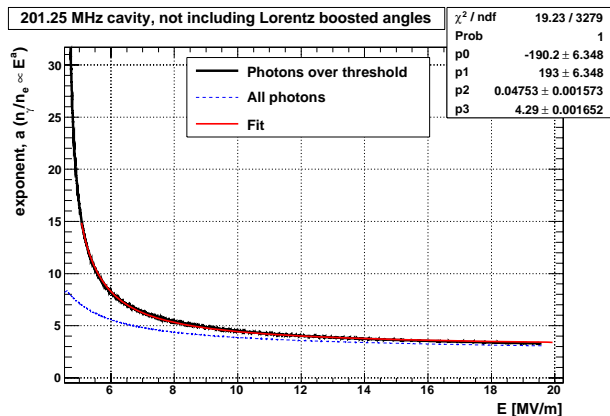


Figure 2: The exponent  $a_{n_\gamma/n_e}$  in for the photon to electron ratio as a function of the acceleration gradient  $E_{acc}$ . The solid black line is taking a detector threshold of 0.42 MeV into account, while the dashed blue line is for photons at any energy.

These effects together produce an effective number of photons at the detector per emitted electron which is proportional to  $E_{acc}^a$ , where  $a$  is a gradient dependent exponent. The value of  $a$  is shown in Fig. 2 as a function of the field gradient. Since the calculations are time consuming and non-trivial, the expression

$$a_{n_\gamma/n_e} = 193.0 e^{0.0475/(E-4.290)} - 190.2 \quad (6)$$

can be used for a 201.25 MHz cavity with this specific geometry.

### Angular Distribution

The bremsstrahlung photons are assumed to be emitted isotropically in the center of mass frame. In the lab frame, Lorentz boost gives more photons in forward direction. Since an electron typically undergoes multiple ionisation interactions with the matter before a photon is produced via bremsstrahlung, the magnitude of the boost is subject to stochastic effects. The forward focussing effect is also reduced by scattering of the electron prior to bremsstrahlung interaction. For these reasons, this phenomenon was simulated in Geant4 and the result is illustrated in Fig. 3. It was concluded that the Lorentz boost gives a modest contribution of  $a_\theta \approx 0.3$  to the photon to electron ratio.

### Comparison with Geant4

In order to verify the calculations of the photon to electron ratio, several million electrons were simulated

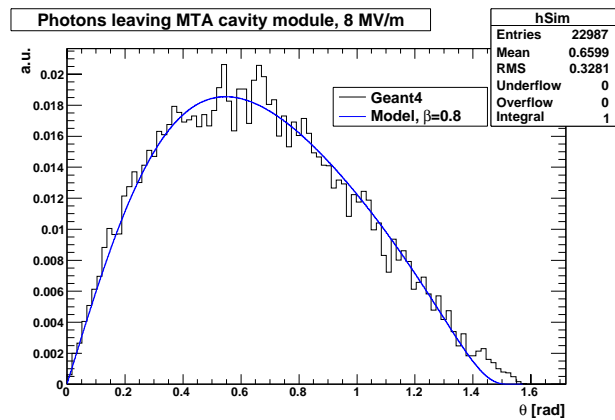


Figure 3: The angular distribution of photons leaving the aluminum plate of the MTA 201.25 MHz cavity. The blue line (not a fit) is the expected distribution if the photons are emitted isotropically in a commoving frame at  $0.8c$ .

in Geant4.8.1 at energies corresponding to 8, 10.5 and 20 MV/m accelerating gradient. Photons were counted at 4.4 m distance on-axis in a 10 cm radius disk. The 8 MV/m simulation found 23 photons, while 21.4 were predicted based on calculations. The corresponding values for 10.5 MV/m were 62 observed and 65.5 predicted, while for 20 MV/m 352 photons were observed and 685 predicted. Hence the agreement is good for  $T \approx 1$  MeV, but at higher energies the model overestimates the photon rates. This is in part due to that energy straggling gives a small chance for the electron to reach the aluminum where the radiation yield is lower than in copper, but mostly due to that Eq. (5) implicitly assumes that all radiation comes from one photon. With increasing energy however, an increasing fraction of the radiation comes from multiple low energy photons which are killed by the photoelectric effect.

### Implications to MICE

According to MTA measurements of the 201.25 MHz cavity, there are  $n_\gamma = 4.03 \cdot 10^{-5}$  photons per RF period<sup>1</sup> at 8 MV/m. This value divided by the calculated  $n_\gamma/n_e = 6.08 \cdot 10^{-8}$  resulted in  $n_e = 662$  electrons emitted from the cavity per RF half period. The MICE experiment [6] uses two linacs of four 201.25 MHz cavities each, operating at 8 MV/m peak field. With two half periods per period, the total number of emitted electrons is  $n_e(\text{MICE}) = 2.13$  THz. A liquid hydrogen absorber with double aluminum windows is placed between a linac and a tracker. Simulations resulted in an overall photon to emitted electron ratio in MICE equal to  $n_\gamma/n_e(\text{MICE}) = 8.315 \cdot 10^{-4}$  [7] for the most exposed tracker reference plane. Hence the photon rate in the tracker reference plane is approximately 2 GHz, which poses a challenge to the trackers and time of flight detectors.

<sup>1</sup>This was derived from data collected during the 88.6  $\mu\text{s}$  long RF flat top, not the full 125  $\mu\text{s}$  long pulse.

## ELECTRON EMISSION RATE

If the surface field gradient is increased, asperities at subsequently lower  $\beta_{FN}$  become “activated” as  $E_{local}$  approaches the field emission region. If the local gradient is too large the asperity is destroyed in a breakdown event [2]. Since Eq. (1) depends very strongly on  $E_{local}$  in the GV/m region, the range of active  $\beta_{FN}$  should thus be very narrow. This is also what is observed [2].

The measurement [1] of the density of asperities was obtained by comparing the accelerating gradient which produced spots of equal intensity. By assuming that breakdown occurred at local gradient  $E_{bd} = 8$  GV/m, reference [1] deduced that the density is proportional to  $e^{-0.027\beta_{FN}}$  for the 805 MHz cavity. The effective electron emission rate  $n_e$  during conditioning can thus be expressed as

$$n_e(E_{acc}) \propto n_e^{FN}(E_{surf}) \int_1^{\beta_{bd}} e^{-0.027\beta_{FN}} d\beta_{FN} \quad (7)$$

where  $E_{surf} = 2.6E_{acc}$  [8] and

$$\beta_{bd}(E_{acc}) = \frac{E_{bd}}{E_{surf}} \quad (8)$$

is the maximum field enhancement of an asperity which is not destroyed in a breakdown event at  $E_{bd}$ .

This hypothesis can be tested by comparing it to the rates measured during conditioning of the 805 MHz cavity. At the maximum accelerating gradient of approximately 20 MV/m, an  $E^{9.5-10}$  dependence was found [8]. The model presented here estimated  $E^{9.7}$  when both electron emission and photon to electron ratio<sup>2</sup> were accounted for.

After conditioning, the density of emitters follows [2]

$$\rho(\beta_{FN}) \propto \frac{e^{-b\beta_{FN}}}{e^{(b\beta_{FN}-\beta_{eq})/d}-1}, \quad \beta_{eq} \equiv \beta_{bd}(E_{acc}^{max}) \quad (9)$$

where  $d$  gives the width of the region where asperities are destroyed. The MTA 201.25 MHz cavity was fully conditioned at  $E_{acc}^{max} = 21$  MV/m. The other constants are unknown<sup>3</sup>, but using  $b = 0.027$  and  $d = 70$  in combination with the photon to electron ratio yielded  $\chi^2/\text{ndf} = 1.29/5$  ( $p = 0.94$ ) when compared with data. The value of  $d$  influences the scaling with the gradient. Fig. 4 illustrates this for  $d \rightarrow \text{inf}$ , the unconditioned case ( $p = 0.66$ ).

## SUMMARY

The model presented here successfully reproduces the observed radiation levels as function of accelerating gradient for RF cavities. The most important factors are the field emission of electrons, the acceleration of these electrons and the subsequent creation of bremsstrahlung photons. This model should be universally applicable, though the parameter values depend on the cavities studied and on

<sup>2</sup>Assuming a very low detector threshold, and that the geometries outside the two cavities are comparable.

<sup>3</sup>Values from the 805 MHz cavity [1, 2, 8] was used when available.

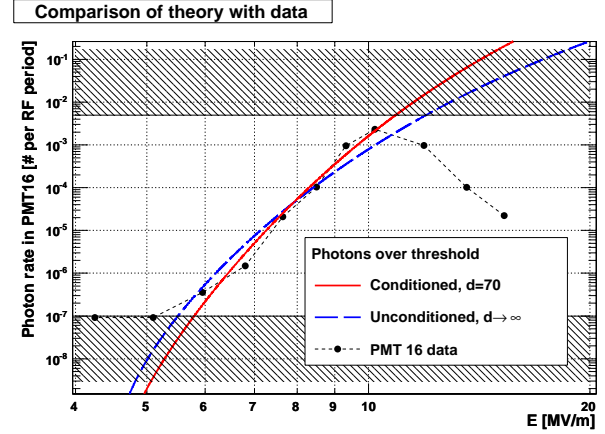


Figure 4: Predicted photon rates compared with experimental data as function of gradient for a fully conditioned 201.25 MHz cavity. At low gradients the data is dominated by noise and cosmic background, and the detector is saturated at high gradients.

the surrounding material. The rates observed in the MTA confirms that the RF induced background poses a challenge to the MICE experiment.

## ACKNOWLEDGEMENTS

The author would like to thank the MuCool collaboration for the free exchange of information and data. University of Geneva has funded this research, and NIKHEF in Amsterdam has provided the means for participation in this conference.

## REFERENCES

- [1] A. Moretti et al. Effects of high solenoidal magnetic fields on rf accelerating cavities. *Phys. Rev. ST Accel. Beams*, 8:072001, 2005.
- [2] A. Hassanein et al. Effects of surface damage on RF cavity operation. *Phys. Rev. ST Accel. Beams*, 9:062001, 2006.
- [3] J. Norem et al. The Radiation Environment in and near High Gradient RF Cavities. Presented at IEEE Particle Accelerator Conference (PAC2001), Chicago, Illinois, 18-22 Jun 2001.
- [4] W. M. Yao et al. Review of particle physics. *J. Phys.*, G33:1-1232, 2006.
- [5] S. M. Seltzer and M. J. Berger. Bremsstrahlung spectra from electron interactions with screened atomic nuclei and orbital electrons. *Nuclear Instruments and Methods in Physics Research B*, 12:95-134, August 1985.
- [6] R. Sandstrom. Status of MICE, the international Muon Ionization Cooling Experiment. *AIP Conf. Proc.*, 981:107-111, 2008.
- [7] R. Sandstrom. Simulation of RF induced background in the MICE experiment. *Nucl. Phys. Proc. Suppl.*, 149:301-302, 2005.
- [8] J. Norem et al. Dark current, breakdown, and magnetic field effects in a multicell, 805 MHz cavity. *Phys. Rev. ST Accel. Beams*, 6:072001, 2003.